Journal of
Manufacturing and Materials Processing

MDPI

Article

A Comparative Study of Non-Destructive Testing Techniques: Active Thermography versus Shearography for 3D-Printed Thermoplastic Composites Reinforced with Continuous Carbon Fiber

Imi Ochana [1,2], François Ducobu [2], Mohamed Khalil Homrani [2], Arnaud Notebaert [1] and Anthonin Demarbaix [1,*]

[1] Science and Technology Research Unit, Haute Ecole Provinciale de Hainaut Condorcet, Boulevard Solvay 31, 6000 Charleroi, Belgium; imi.ochana@condorcet.be (I.O.); arnaud.notebaert@condorcet.be (A.N.)
[2] Machine Design and Production Engineering Lab, Research Institute for Science and Material Engineering, University of Mons, 7000 Mons, Belgium; francois.ducobu@umons.ac.be (F.D.); mohamedkhalil.homrani@umons.ac.be (M.K.H.)
* Correspondence: anthonin.demarbaix@condorcet.be

Abstract: This study investigates the feasibility and effectiveness of two non-destructive testing methods, active thermography and shearography, on 3D-printed thermoplastic (TP) composites reinforced with continuous carbon fiber. Artificial defects were introduced into the composite plate to benchmark the detection capabilities of these non-destructive testing techniques (NDT). Active thermography produced a thermogram that highlighted defects through variations in surface temperature. Although effective for identifying defects ranging from 3 to 10 mm in size at four different depths, specifically 1 mm, 1.25 mm, 1.5 mm, and 1.75 mm, through the thickness of a 2.8 mm plate, the method encountered some limitations. It faced challenges in detecting deeper defects and accurately determining their shapes. Shearography, which utilizes fringe pattern distortions to detect surface displacement anomalies, successfully identified near-surface defects within the same size range. However, it required more expertise for accurate interpretation and struggled with detecting smaller and deeper defects. The complementary strengths and limitations of these methods suggest that employing both could offer a more comprehensive solution for defect detection in 3D-printed TP composites.

Keywords: active thermography; shearography; 3D printing; continuous carbon fiber

Citation: Ochana, I.; Ducobu, F.; Homrani, M.K.; Notebaert, A.; Demarbaix, A. A Comparative Study of Non-Destructive Testing Techniques: Active Thermography versus Shearography for 3D-Printed Thermoplastic Composites Reinforced with Continuous Carbon Fiber. *J. Manuf. Mater. Process.* **2024**, *8*, 227. https://doi.org/10.3390/jmmp8050227

Academic Editor: Sharifu Ura

Received: 30 August 2024
Revised: 7 October 2024
Accepted: 9 October 2024
Published: 11 October 2024

1. Introduction

Over the past decades, 3D-printed TP composites have gained popularity across various industrial sectors. Whether in aerospace, automotive, healthcare, or energy, 3D-printed TP composites are revolutionizing the way we design and manufacture parts and structures [1]. Additive manufacturing (AM) allows for greater precision in complex structures compared to traditional manufacturing methods. Very fine and intricate structures can be built layer by layer. AM also enables the repair of high-value components, providing an economical and sustainable solution for numerous industries. The mechanical properties of components produced by AM are comparable to, and in some cases exceed, those of conventionally treated structures [2]. These composite materials offer a unique combination of lightness, mechanical strength, and flexibility, making them suitable for a variety of applications. Their ability to be customized, reduce waste, and accelerate production cycles makes them an attractive solution for many industries [3]. TP matrix composites offer several significant technological advantages. Firstly, the unlimited shelf life of the polymer under normal storage conditions is a major benefit compared to thermoset (TS) composites. Additionally, manufacturing time is significantly reduced due to the absence of the lengthy polymerization process associated with TS matrices. Furthermore, the ability to shape the

material in its heated state and its reprocessability make it a versatile solution for various industrial applications [4].

A recent advancement in the field of additive manufacturing of composites is the development of coextrusion technology by Anisoprint, particularly in the context of fused deposition modeling (FDM) [5]. Coextrusion involves the simultaneous deposition of two materials: a filament of continuous fiber pre-impregnated with a thermoset resin, which is CFRTS, and a TP matrix. Both materials enter the nozzle where the TP is heated, becoming malleable, and it effectively envelops the CFRTS filament as illustrated in Figure 1a. This process results in the CF, already embedded in the TS matrix, being further coated by the TP material, creating a CFRTSTP filament. This integrated approach ensures that the reinforcing carbon fiber, already embedded in the thermoset matrix, is precisely aligned with the thermoplastic during the printing process, which enhances the mechanical properties and dimensional accuracy of the printed parts [6]. Unlike dual-nozzle systems, illustrated in Figure 1b, where TP and CF are deposited separately, coextrusion combines the CFRTS filament and the TP filament into a single step, resulting in a composite with a TS matrix around the fiber and a TP matrix around the entire structure. This leads to improved structural integrity and strength of the final composite [7]. The coextrusion method not only streamlines the printing process but also reduces the risk of fiber misalignment, which can compromise the performance of the printed component. By using a pre-impregnated fiber, coextrusion ensures that the fiber–matrix interface is optimized for high performance, while the outer TP matrix provides additional strength and processability. Coextrusion is therefore a critical innovation for producing high-quality CFRTP composites with superior mechanical properties and precision [8].

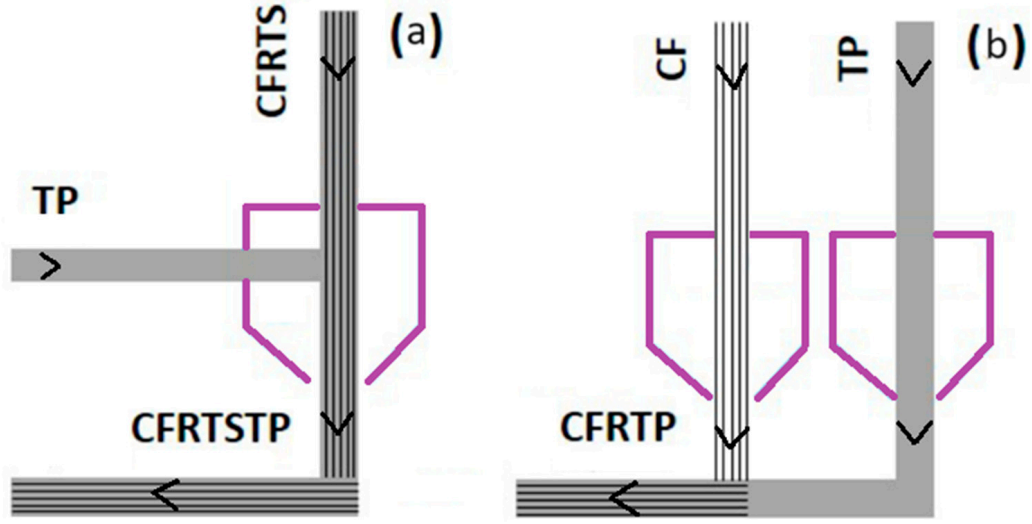

Figure 1. Coextrusion versus dual-nozzle technologies: (**a**) thermoplastic (TP) is melted with continuous-fiber-reinforced thermoset (CFRTS) in the nozzle creating continuous-fiber-reinforced thermoset–thermoplast (CFRTSTP) filament; (**b**) continuous fibers (CF) are added after thermoplastic (TP) creating continuous-fiber-reinforced thermoplastic (CFRTP) filament.

In a recent study, Demarbaix et al. [5] explored the feasibility of printing self-sensing composite parts using continuous carbon fiber. They demonstrated the potential of coextrusion technology to produce parts that not only meet structural requirements but also have integrated sensing capabilities, useful in applications like structural health monitoring (SHM) [6] and soft robotics. The study highlights the advantages of using continuous fibers for both mechanical reinforcement and electrical conductivity, which can be monitored in real time to predict material failure. This research underscores the importance of coextrusion in advancing multifunctional 3D printing technologies [5].

However, several factors hinder the growth of this market: material characterization during development, process control, and integrity assurance [7]. The use of non-destructive testing (NDT) [8] is essential to ensure the quality and reliability of 3D-printed continuous carbon fiber composites. These inspection techniques enable the properties of parts to be assessed without altering their mechanical integrity, thereby reducing costs and boosting confidence in inspection processes. By detecting defects such as cracks, voids, inclusions, and porosity at an early stage, NDT helps to avoid costly repairs or subsequent replacement. It is essential to ensure that products meet the required quality standards and guarantee user safety. Among the methods particularly well-suited for inspecting these materials are radiographic testing, computed tomography, ultrasonic testing, infrared thermographic testing, and shearography [9]. Radiographic testing (RT) employs X-rays or gamma rays to detect internal defects such as delaminations. Computed tomography, also using X-rays, provides detailed cross-sectional images for a comprehensive view of internal anomalies. Ultrasonic testing, which uses ultrasonic waves, is effective for identifying delaminations and density variations, and is widely used for quality control of composites. Infrared thermographic testing detects surface and near-surface defects by measuring temperature variations, often caused by irregularities in the material's thermal conductivity. Shearography identifies defects by analyzing deformation patterns under stress, making it particularly useful for detecting subsurface flaws like delaminations and voids.

Numerous studies have already compared various NDT technologies, such as thermography and shearography, to demonstrate their effectiveness in inspecting composite materials obtained by classical manufacturing processes. Georges et al. [10] compared thermography and shearography on a hybrid sandwich metal-composite flat panel. Thermography, using lamp heating, detects defects up to 2 mm deep, with diameters as small as 6 mm. In contrast, shearography yields good results for larger defects such as 25 mm air gaps at depths less than 2 mm. Garnier et al. [11] studied the comparison between shearography and thermography for the inspection of an epoxy/carbon composite plate. They found that shearography shows variations of 8% in length and 21% in width compared with the reference measurement, while induction thermography shows variations of 12% in length and 20% in width. Wei et al. [12] explored the efficiency of long pulse thermography (LPT) and shearography in detecting defects in carbon-fiber-reinforced polymers (CFRP) and aluminum honeycomb panels. Their study demonstrated that LPT is particularly effective for CFRP, providing high accuracy with minimal error for small defect detection. However, in aluminum honeycomb panels, shearography performed better, effectively identifying all pre-embedded debonding defects. They concluded that combining both methods could optimize defect detection across different materials. Hung et al. [13] examined the application of thermography and shearography in evaluating fiber-reinforced composites. Their research highlighted that thermography effectively locates adhesive bond defects, while shearography is advantageous for identifying deformations caused by internal flaws under stress. They concluded that a combined approach enhances defect detection reliability, compensating for the limitations of each method when used alone. However, none of these studies have addressed 3D-printed composites. To date, no articles have been found comparing shearography and thermography on 3D-printed composite parts. Thermoplastic-based composites are gaining increasing prominence in various industries due to their recyclability, toughness, and ease of processing. As the use of 3D printing for manufacturing composite materials grows, especially for complex and customizable components, it is essential to assess the effectiveness of NDT methods on these new materials. Since TP can exhibit different behavior compared to traditional TS composites, understanding how these NDT techniques perform in this context is crucial for ensuring the quality and reliability of 3D-printed parts.

Building upon these findings, the aim of this project is to compare the efficacy of active thermography and shearography on a 3D-printed composite plate reinforced with continuous carbon fiber, in which artificial defects with defined geometries have been integrated. Although defects such as porosity and cracks can occur in 3D-printed parts reinforced

with continuous fibers, this study focuses mainly on the analysis of artificial defects in the form of voids deliberately inserted into the plate in order to assess the performance of non-destructive testing methods. The two non-destructive testing methods were selected for comparison due to their shared principle of using an external excitation source, specifically heat, to induce detectable changes in the test material. Both methods involve the application of thermal energy to the plate, followed by the capture of resultant responses via imaging systems. In active thermography, the infrared camera records the thermal radiation emitted from the surface of the plate as it heats up and cools down, enabling the identification of temperature anomalies associated with defects. In shearography, the application of heat introduces slight variations in the material's internal stress state, which are captured by a shearography camera. The camera monitors changes in the optical phase of light reflected from the surface during the cooling phase, revealing the presence of subsurface defects. The comparison of these two technologies offers insights into their respective strengths and limitations in defect detection. While both rely on heat as the excitation source, they differ in how the material's response is captured: thermography detects variations in surface temperature patterns, whereas shearography measures local strain variations by capturing changes in the fringe patterns that correspond to the mechanical response of the material under thermal excitation. These two non-destructive testing techniques will be evaluated to detect and characterize defects in the plate. The limitations and potential advantages of both inspection techniques will be discussed.

2. Materials and Methods

This section discusses the materials and methods employed in this study. The focus will first be on the benchmark composite plate, detailing its composition and manufacturing process. Following this, the non-destructive methods used to evaluate the integrity of the composite benchmark will be explored.

2.1. The Benchmark

In the context of this study, a composite plate made of continuous-carbon-fiber-reinforced thermoplastic polymer is used as a benchmark, manufactured by 3D printing using the FDM method. This plate was printed with the Anisoprint Composer A4 printer, which is characterized by its coextrusion technology. The benchmark used in this study is based on the plate model proposed by Saeed et al. [14]. This rectangular plate measures 220 mm in length, 140 mm in height, and has a thickness of 2.8 mm. It consists of 8 plies arranged in a sequence of $(0/45/90/-45^{\circ})_2$ orientations. The plate contains 16 internal defects of various sizes and shapes, the exact dimensions of which are given in Figure 2, and these defects are located at different depths. To create these defects, the printing head does not deposit material at the locations of the defects to reproduce any delamination or porosity present in real components. The geometric model of the benchmark used can be seen in Figure 2.

The accurate fabrication of this benchmark plate is essential for validating the results of the following NDT methods.

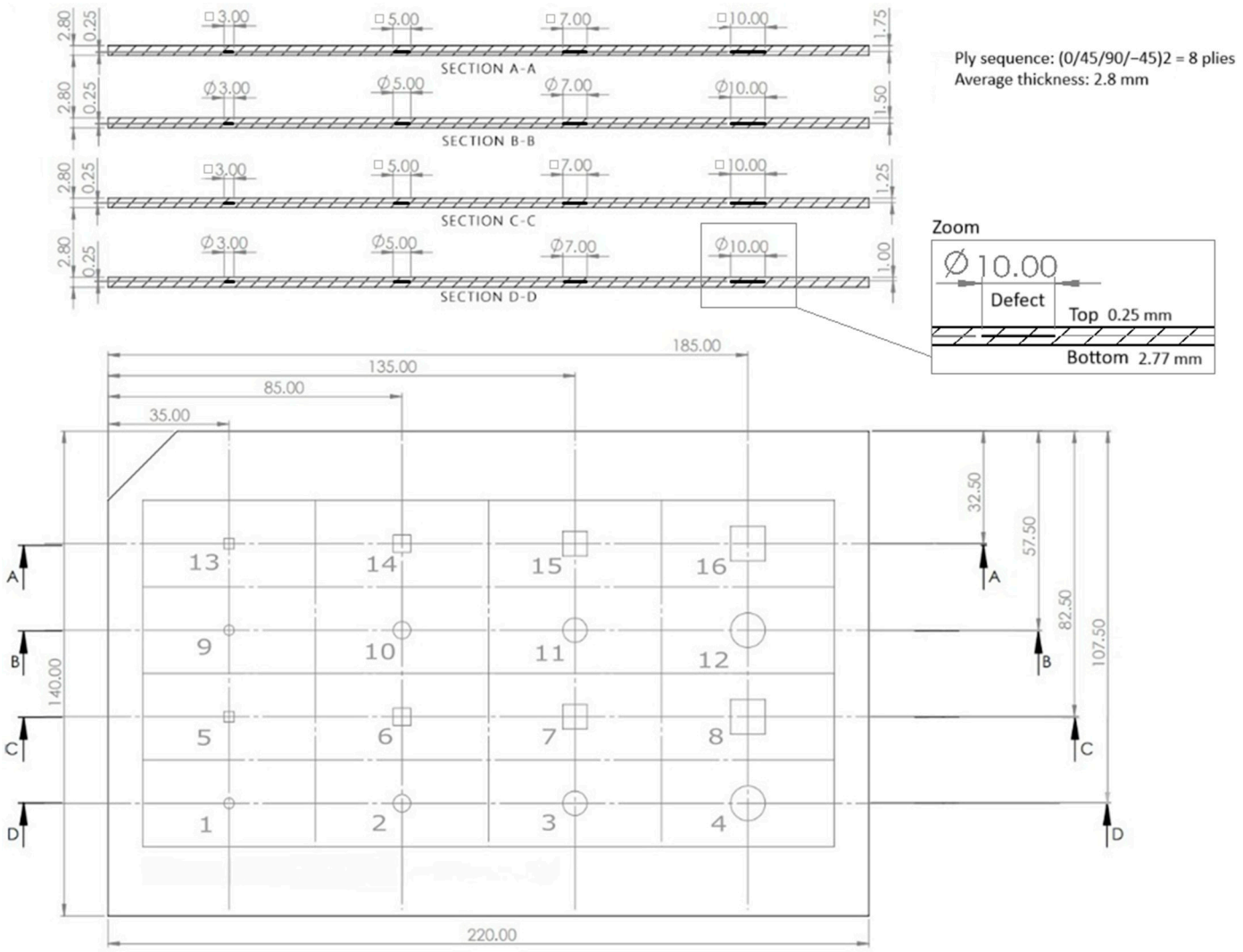

Figure 2. Benchmark geometry and specifications.

2.2. Non-Destructive Testing Methods

The RT method, using the X-RIS Dxbox-200 X-ray Inspection Cabinet from WAN, Charleroi, Belgium, was utilized as a preliminary step to verify the presence and location of any pre-existing defects in the specifically designed benchmark. This reference plate serves as a control, allowing for a clear and reliable comparison of defect detection capabilities between the active thermography and shearography methods on 3D-printed composite reinforced with continuous carbon fiber. The radiographic image of the reference benchmark plate, illustrating the identified defects, is presented in Figure 3.

The defects numbered 1 to 4, located at a depth of 1 mm from the top surface of the plate, are clearly visible. Their dimensions and the shape of the defects can be determined with precision. Similarly, the defects numbered 5 to 8, located at a depth of 1.25 mm from the top surface of the plate, are also clearly visible. Their dimensions and shape can be accurately determined. In contrast, the defects numbered 11 and 12 (at a depth of 1.5 mm) and 15 and 16 (at a depth of 1.75 mm) are discernible, but it is difficult to distinguish whether they are circular or square in shape. Additionally, their dimensions are challenging to measure accurately. Finally, the defects numbered 9 and 10 (at a depth of 1.5 mm) and 13 and 14 (at a depth of 1.75 mm) with dimensions below 5 mm, are not detectable in the radiographic image.

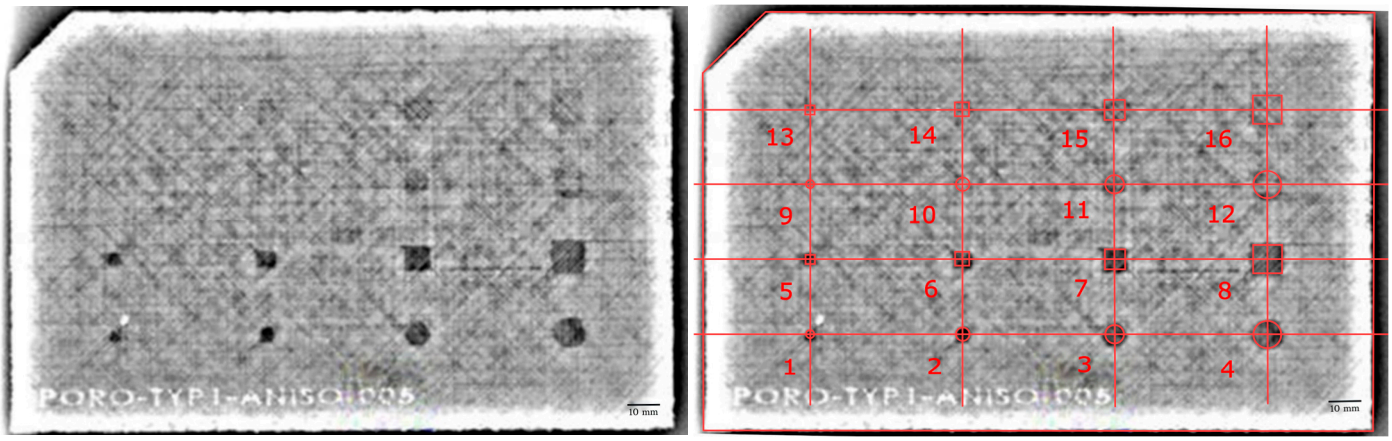

(**a**) (**b**)

Figure 3. Radiographic result of the reference benchmark: (**a**) X-ray image of the 3D-printed composite plate; (**b**) overlay of defect map on the X-ray image. This image shows the same plate with a red overlay indicating the positions and numbers of the artificial defects introduced.

By confirming the presence of defects in the reference benchmark plate, the RT method establishes a baseline for the experimental study. This baseline ensures that any defects identified in subsequent tests on the composite plate are genuine and not the result of inconsistencies introduced during the manufacturing process or inaccuracies in the test setup. Consequently, this RT verification guarantees the integrity of the benchmark plate, making it a reliable standard for comparison.

To accurately assess and detect defects or anomalies within the test plate, two complementary NDT methods were employed: active thermography and shearography. Active thermography is a technique that involves heating the surface of the material to be inspected and measuring its temperature evolution using an infrared camera. During the control, the object of study is scanned using an infrared camera to measure the surface temperature. This technology is based on the physical principle that each body diffuses a certain amount of electromagnetic radiation which is determined by its emissive power. Infrared thermography allows temperature measurements to be taken from a distance, without contact, by detecting the object's or target surface's own infrared emissions. [13]. Thermography has the capability to detect some defects that are located deeper within the material, providing a comprehensive assessment of the object's integrity [15]. Shearography, also referred to as speckle-pattern shearing interferometry, is a non-destructive testing technique that employs the principles of coherent laser light, akin to holographic interferometry. This method is used to generate a visual representation of an object under testing, facilitating the detection of various defects in metallic and composite materials. The shearography process starts with capturing an image of the test object in its unloaded or neutral state. The reflected light from the surface, if not entirely smooth, results in a speckle pattern, which is recorded by the camera. Subsequently, the object is subjected to stress or excitation, typically through mechanical load or thermal heating. This induces a reaction in the material, causing any existing defects to expand. Following the application of stress, a second image is captured, representing the deformed state of the object. The speckle pattern in this image differs from the initial one. The subsequent analysis involves the subtraction of the second image from the first, resulting in a shearographic fringe pattern, or shearogram [16]. This pattern delineates the topography of surface defects, including but not limited to cracking, disbonding, delamination, fluid ingress, porosity, and wrinkling [17]. The characteristic black and white fringe pattern provides valuable insights into the relative deformation of the inspected object. In the absence of defect features, the pattern appears regular. However, a disturbance in the pattern indicates the presence of a subsurface defect. This technique, therefore, not only facilitates defect

identification but also enables the measurement of deformation extent in composites and metallic materials [18].

Following the explanation of the active thermography and shearography techniques, their experimental setup is presented below. As shown in Figure 4a, both methods share a nearly identical configuration. In this setup, α represents the orientation of the halogen lamps in the horizontal plane, L is the distance between the camera and the sample, and d is the distance between the camera and the halogen lamp.

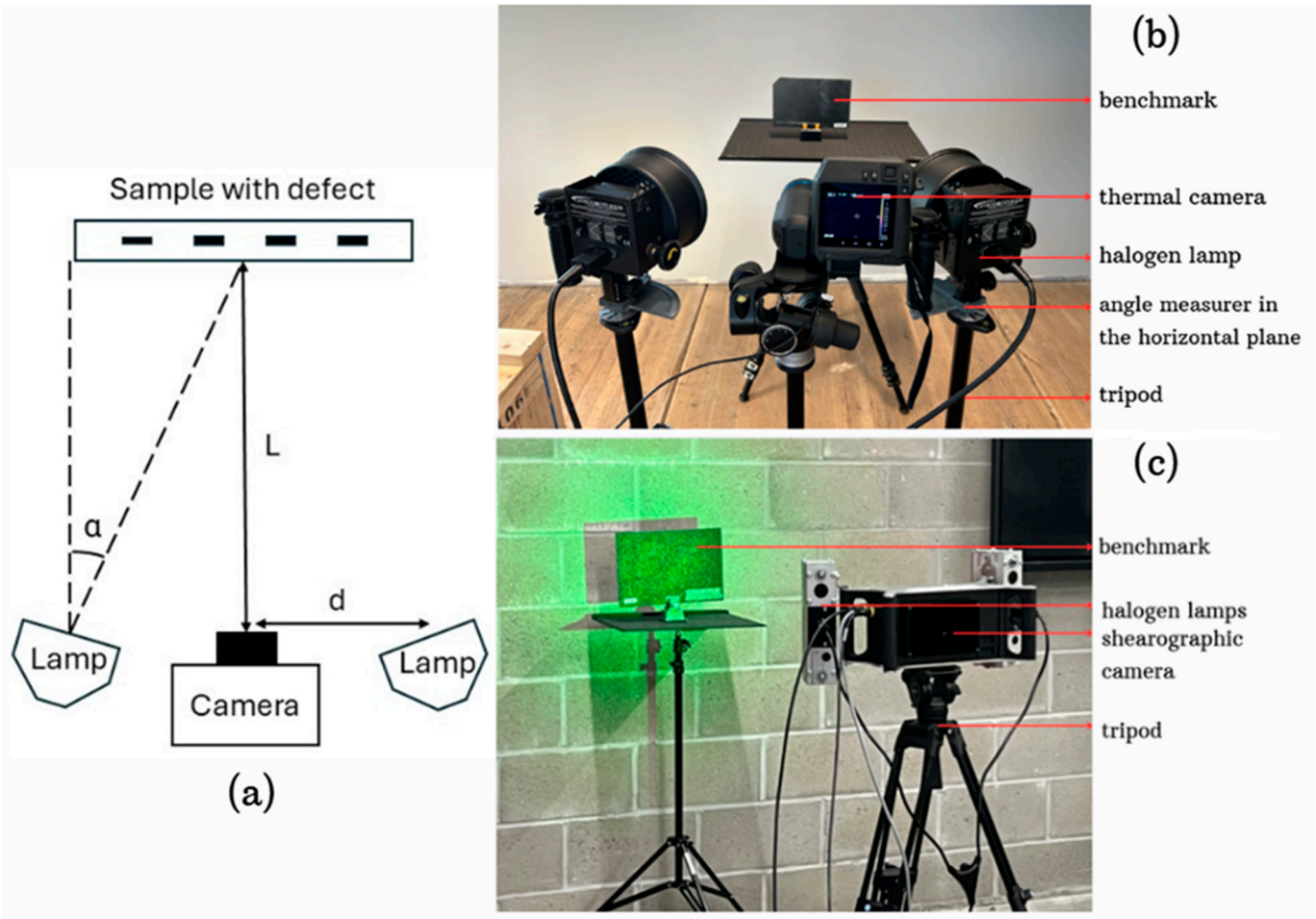

Figure 4. Experimental setup of non-destructive techniques: (**a**) schematic of general setup; (**b**) active thermography setup; (**c**) shearography setup.

The experimental setup for active thermography includes two halogen lamps mounted on tripods, each with a power output of 1000 W, which serve as the thermal source. A FLIR T560 infrared camera, equipped with a 17 mm focus lens, is positioned at a distance from the test plate to capture the thermal images effectively. This setup is optimized to ensure uniform heating of the plate, which facilitates accurate defect detection through thermal imaging. The adjustable parameters of the configuration, summarized in Table 1, include the distance between the thermal source and the plate, the angle of the lamps, the exposure time, and the positioning of the camera relative to the test object.

This configuration is designed to deliver consistent and even heat distribution across the surface of the plate, enabling the infrared camera to capture detailed thermal variations associated with defects. The spatial arrangement of the camera, heat sources, and sample is visually represented in Figure 4b.

Table 1. Adjustable parameters of the experimental setup of thermography tests [19].

Symbols	Parameters	Value
L	Distance between thermal source and plate	70 cm
a	Angle of lamps relative to plate	20°
d	Distance between lamps and camera	30 cm
t	Exposure time	10 s

Regarding shearographic tests, Table 2 outlines the experimental parameters that were selected to conduct the measurements. The parameter Ds represents the shearing distance, which is a parameter of the shearographic camera. It is the distance between two points on the surface of the object that are compared to detect deformations.

Table 2. Parameters of the experimental setup of shearography tests.

Symbols	Parameters	Value
L	Distance between thermal source and plate	1 m
a	Angle of lamps relative to plate	20°
d	Distance between lamps and camera	30 cm
D_S	Shearing distance	7 mm

Several experimental trials were conducted to determine the optimal parameters for maximizing the accuracy of defect detection in the tested composite plates. Each trial involved adjustments to the parameters, such as the exposure time, which affected the final temperature of the plate, the distance between the camera and the plate, and the shearing angle. The inputs of experimental configurations are summarized in Table 3.

Table 3. Inputs and results of shearography tests for defect detection.

Inputs	Trial 1	Trial 2	Trial 3	Trial 4
Shearing angle (°)	45	0	90	45
Exposure time (s)	45	15	15	15
Results				
Final temperature of the plate (°C)	30	27	27	27

For the first trial, the exposure time was set at 45 s, which allowed the plate to be heated to a final temperature of 30 °C. However, after analysis, it was determined that heating the plate for only 15 s already allowed a temperature of 27 °C to be reached, which is the minimum temperature to highlight the majority of defects in a single shot. Therefore, for the following tests 2, 3, and 4, the exposure time was reduced to 15 s, thus maintaining a stable temperature of 27 °C on the plate.

Another parameter modified in the tests is the shearing angle. In the first trial, this angle was 45°. In the second trial, the angle was adjusted to 0°, and in the third one, it was changed to 90°. In the end, the 45° shear angle showed the greatest number of defects in a single image. The other parameters, such as the distance between the camera and the plate and the shear distance, remained constant throughout the four tests.

Trial number 4 was identified as the optimal setup for defect detection. This choice is explained by the combination of parameters that yielded the best results in terms of image accuracy and clarity. During this trial, the plate was heated for 15 s, allowing its temperature to stabilize at 27 °C, an ideal value for generating the necessary thermal deformations for defect detection. The Optrion camera was positioned one meter away from the plate, capturing images with sufficient resolution to observe deformations during both the heating and cooling phases. The shearing angle was set at 45°, while the shearing distance was 7 mm. This configuration, illustrated in Figure 4, provided an optimal field of view for detailed deformation analysis, thus improving defect detection.

3. Results

In this study, the two non-destructive testing methods presented in the previous section, active thermography and shearography, were applied to the 3D-printed composite plate. This benchmark was used as a reference to compare the effectiveness of these two methods in detecting defects. The main objective was to determine the feasibility and comparative effectiveness of active thermography and shearography on 3D-printed composite materials reinforced with continuous carbon fiber. The results obtained revealed detailed information on the presence of defects detected by each method, providing indications of their respective effectiveness. The specific details of these testing methods, the corresponding results, and their comparison are presented in this section.

3.1. Active Thermography

To begin with, Figure 5 presents the results obtained for the active thermography tests.

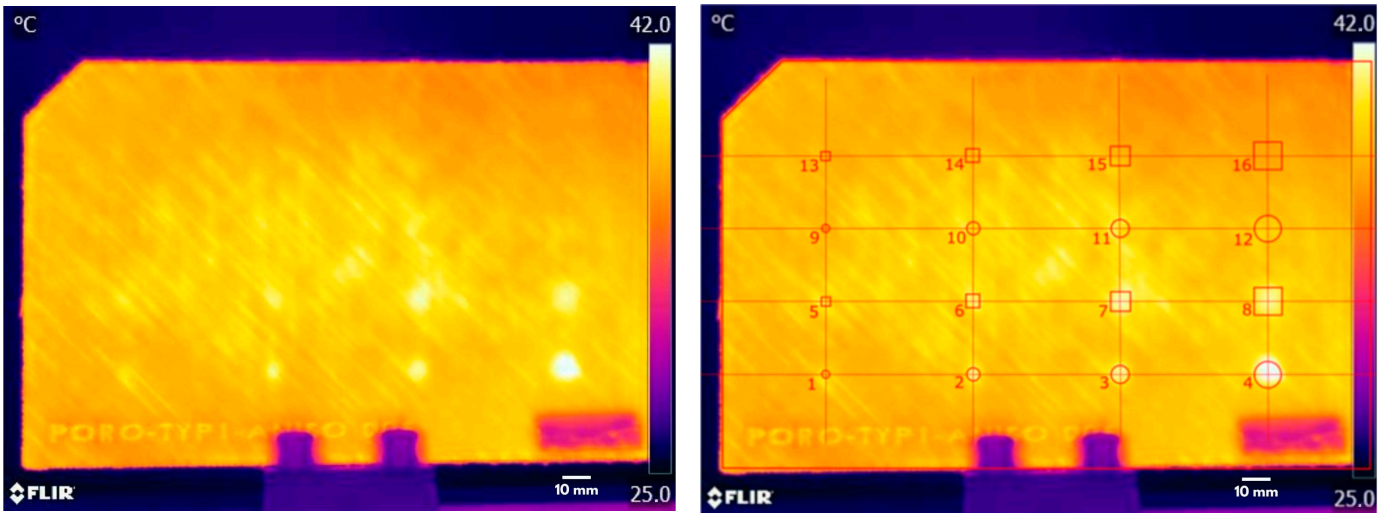

(**a**) (**b**)

Figure 5. Active thermography results: (**a**) thermogram of the 3D-printed composite plate. This image shows the temperature distribution on the surface of the plate after applying the active thermography method. (**b**) Overlay of defect map on the thermogram. This image shows the same plate with a red overlay indicating the positions and numbers of the artificial defects introduced.

The analysis of the thermogram in Figure 5a reveals several hot and cold spots indicating thermal anomalies potentially related to the presence of internal defects. To better understand these anomalies, the defect map is superimposed on the thermogram in Figure 5b. The numbered areas in Figure 5b correspond to the artificial defects introduced in the composite plate. Figure 6 illustrates the outcomes of active thermography analysis after post-processing techniques were applied to enhance defect detection. Compared to the raw data presented in Figure 5a, this image demonstrates a significant improvement in identifying the various defects within the material. Indeed, in the raw image, only defects 3, 4, 7, and 8 are visible. However, in the post-processed image, both of the first two rows corresponding to defects 1 to 8 are clearly visible.

To provide further detail from the post-processing thermogram, the visible defects include:

- Defects 1 to 4, which are circular in shape and located at a depth of 1 mm within the plate, with respective sizes of 3 mm, 5 mm, 7 mm, and 10 mm.
- Defects 5 to 8, which have a nominal square shape, are located at a depth of 1.25 mm within the plate, with respective sizes of 3 mm, 5 mm, 7 mm, and 10 mm.

- Additionally, defects 11 and 12, which are circular and located at a depth of 1.5 mm, are less visible than the others but nevertheless are now detectable in the post-processed image.

Conversely, some defects remain undetected:

- Defects 9 and 10, which are circular with respective sizes of 3 mm and 5 mm, and are located at a depth of 1.5 mm.
- Defects 13 to 16, which are square in shape with respective sizes of 3 mm and 10 mm, and are located at a depth of 1.75 mm.

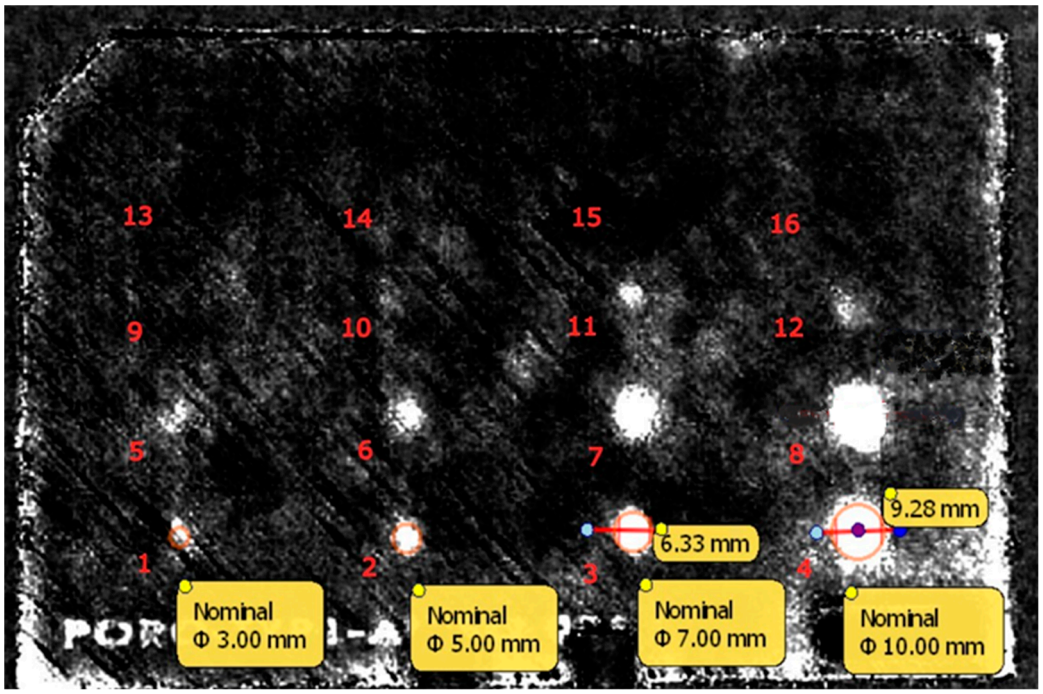

Figure 6. Thermogram post-processing.

To further assess the accuracy of the defect detection, measurements were taken using the Maestro software version 5.14.8. Figure 6 shows both the nominal characteristic lengths of the defects and the measured values obtained through the software. Since the defects have circular or square shapes, their characteristic lengths, diameter for circular defects, and side length for square defects were used for comparison. The percent deviation Δ between the nominal characteristic length and the measured value for each defect was calculated using the following equation:

$$\Delta = \frac{Nominal\ Value - Measured\ Value}{Nominal\ Value} \times 100. \quad (1)$$

Applying Equation (1), the deviations for defects 3 and 4 were determined as follows:

- For defect 3, with a nominal value of 7 mm and a measured value of 6.33 mm, the deviation is 9.57%.
- For defect 4, with a nominal value of 10 mm and a measured value of 9.28 mm, the deviation is 7.2%.

It should be noted that the observed deviations, which are close to 10%, can be attributed either to the inherent limitations of measurement precision, or to transient temperature effects. However, it is important to emphasize that during the thermography tests, the material's glass transition temperature is not reached, eliminating any risk of deforming the part due to heat exposure.

For the remaining defects, accurately defining the measured values using the software proved to be challenging. Firstly, the exact delimitation of the defect area, whether circular or square, proved complex, making it difficult to determine its precise geometry. Secondly, the intensity of the anomalies detected is a delicate factor to analyze. Indeed, some anomalies can be interpreted as defects, but a comparison with other areas of the plate reveals similar intensities without the presence of artificial defects. Thus, only defects 3 and 4 could be effectively quantified.

The post-processing techniques have effectively revealed most defects located at depths up to 1.25 mm. However, detecting defects becomes more challenging as the depth increases, with fewer defects at depths above 1.5 mm being identified. Additionally, smaller defects, particularly those with diameters of 3 mm and 5 mm, are more difficult to detect, especially when located at greater depths. This limitation is mainly due to the thermal diffusion process, which weakens as the depth increases. For deeper defects, the heat generated does not reach the surface as effectively, reducing thermal contrast and making it more challenging to identify the defects. Similarly, smaller defects produce less pronounced thermal variations, further complicating their detection. So, although active thermography can identify certain defects down to a depth of 1.5 mm, accurate defect depth estimation remains limited by thermal diffusion and reduced thermal contrast at greater depths.

The effectiveness of active thermography in this experiment demonstrates its capability to detect and locate internal defects in reinforced composite materials. The thermal variations observed are consistent with the positions of the artificial defects, confirming the sensitivity of this method. Using this experimental setup, the positioning of the defects within the plate was accurately identified. Furthermore, the visible defects, which have sizes ranging from 5 mm to 10 mm, are those located at depths of 1 mm and 1.25 mm in the plate relative to the analyzed surface. However, the exact shape of the defects, whether square or circular, could not be determined.

3.2. Shearography

The series of images presented in Figure 7 corresponds to the results obtained from a shearography inspection. These images illustrate the evolution of wave propagation through the analyzed plate. The wave, highlighted with red circles in each image, enables us to detect and visualize defects within the structure as it moves across the material.

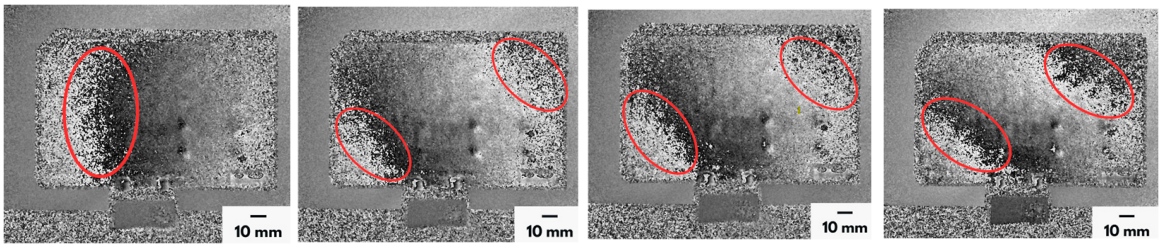

Figure 7. Wave propagation and defect visualization in shearography analysis.

From the sequence of images obtained through the shearography inspection, it was necessary to select a specific image, shown in Figure 8, for detailed analysis. This selection was made to determine the most suitable frame for detecting and assessing potential defects within the material. The choice of image was guided by the clarity of the wave propagation patterns and the contrast between areas of interest.

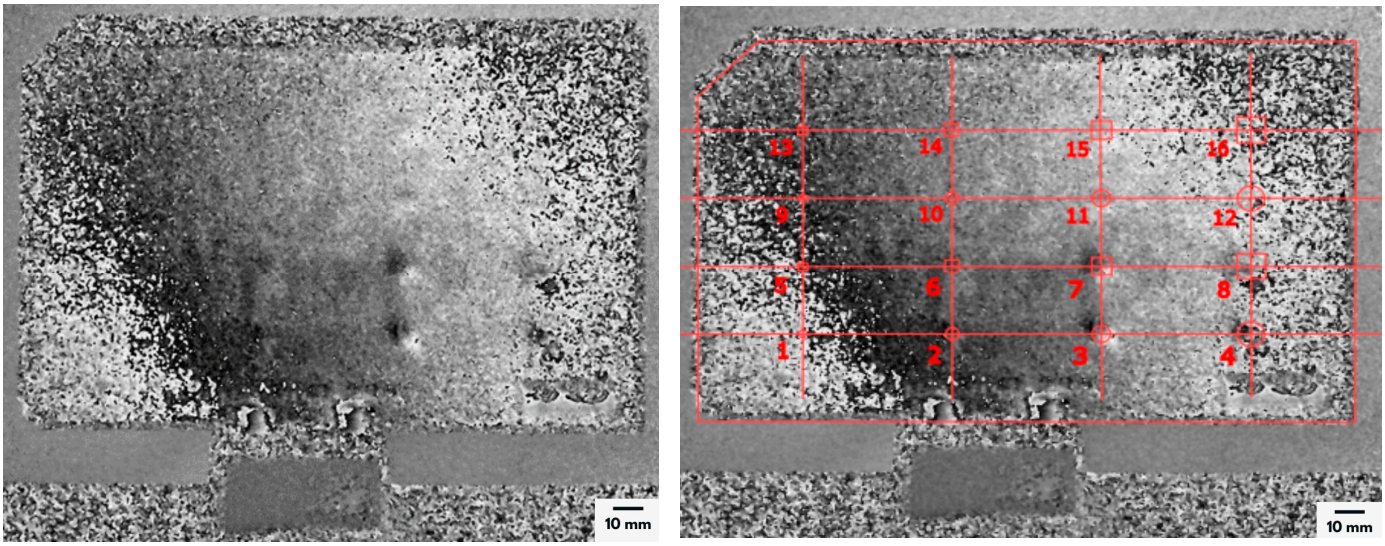

(**a**) (**b**)

Figure 8. Shearography results: (**a**) shearogram of the 3D-printed composite plate. This image shows the interference pattern of the 3D-printed composite plate captured after applying a heating excitation. (**b**) Overlay of defect map on the shearogram. This image shows the same plate with a red overlay indicating the positions and numbers of the artificial defects introduced.

The analysis of the shearogram in Figure 8a reveals several fringe disturbances indicating surface displacement anomalies potentially related to the presence of internal defects. To better understand these anomalies, the grid overlay is applied to the shearogram in Figure 8b. The numbered areas in Figure 8b correspond to the artificial defects introduced in the composite plate. The following observations were made:

- Visible Defects: Defects 3 and 7 are particularly noteworthy. Defect 3, a circular defect with a dimension of 7 mm located at a depth of 1 mm in the plate, shows fringe pattern distortion. Similarly, defect 7, a square defect also measuring 7 mm but located slightly deeper at 1.25 mm, is visible. These defects stand out primarily due to their proximity to the surface, which enhances the visibility of the fringe pattern distortions, despite their not being the largest defects.
- Less Visible Defects: On the other hand, larger defects, such as defects 4 and 8, which have dimensions of 10 mm, exhibit less pronounced thermal variations. Defect 4 is located at a depth of 1 mm within the plate, while defect 8 is situated at a depth of 1.25 mm. Despite their larger size, these defects display only minimal fringe pattern distortions, making them less prominent in the shearographic analysis. One possible explanation for this phenomenon is the influence of edge effects, which can impact the accuracy of defect detection near the boundaries of the plate. As the wave propagates through the material, it interacts with the edges, causing distortions in the wavefront that may reduce the visibility of defects, particularly those located closer to the edges. Furthermore, the dynamics of wave propagation can result in non-uniform visibility of defects at a given moment, as the wave moves through the material. This can lead to situations where larger defects are not as clearly discernible as smaller, shallower defects that may create more immediate surface deformations.
- Non-Visible Defects: Several defects were not detected in the shearographic images. Among these, defects 1 and 2, which are circular in shape with dimensions of 3 mm and 5 mm, respectively, are located at a depth of 1 mm. Defects 5 and 6, which are square-shaped with the same dimensions of 3 mm and 5 mm, are positioned slightly deeper at 1.25 mm. Additionally, defects numbered 9 to 16, found at depths of 1.5 mm or greater, have dimensions ranging from 3 mm to 10 mm but remain undetected. The challenges encountered during these tests include the fact that smaller and deeper

defects induce less surface deformation, leading to minimal or no fringe pattern distortions. The difficulty in detecting these deeper or smaller defects underscores the limitations of the current shearographic setup in identifying internal anomalies, particularly as defect depth increases.

- Out of the sixteen artificial defects introduced in the composite plate, the shearographic analysis detected four defects. Specifically, defects 3 and 4, both circular and located at a depth of 1 mm, with diameters of 7 mm and 10 mm, respectively, and defects 7 and 8, both square and situated at a depth of 1.25 mm, with sizes of 7 mm and 10 mm, respectively, were identified. These results demonstrate the sensitivity of the shearography technique and the current experimental setup in detecting internal defects, particularly those closer to the surface.
- However, it is important to emphasize that the interpretation of images obtained through shearography is challenging. The method's reliance on fringe pattern distortions, which can vary subtly with defect size and depth, complicates the clear identification of all anomalies within a single shearogram. In particular, deeper defects produce weaker fringe distortions, which are more prone to being masked by noise or other surface irregularities. This complexity underscores the need for careful analysis and potential refinement of the technique to improve its effectiveness, especially for detecting deeper or smaller defects.

4. Discussion

Both active thermography and shearography have been used to detect certain internal defects in 3D-printed TP composites reinforced with continuous carbon fiber. However, while these methods have shown some effectiveness, they represent only an initial step in evaluating the material. Not all defects were detected, suggesting that further work is needed. Table 4 provides a comparative summary of the results obtained using both techniques, including the types of defects detected, along with their sizes and depths within the plate. These results give an indication of the current capabilities and limitations of each method.

Table 4. Summary of the results of active thermography and shearography tests for defect detection.

Method	Defect No.	Size of Defect (mm)	Depth of Defect (mm)
Active Thermography	1	3	1
	2	5	1
	3	7	1
	4	10	1
	5	3	1.25
	6	5	1.25
	7	7	1.25
	8	10	1.25
Shearography	3	7	1
	4	10	1
	7	7	1.25
	8	10	1.25

The results obtained from the active thermography technique demonstrate its efficacy in detecting subsurface defects within the composite material. Specifically, the technique identified eight defects, as detailed in Table 4, with a clear distinction between defects located at varying depths and sizes. The post-processing techniques applied to the thermograms significantly improved the visibility of defects, particularly those situated at depths of 1 mm and 1.25 mm. However, defects positioned deeper within the material or those with smaller dimensions, such as 3 mm and 5 mm, proved challenging to detect, especially at depths greater than 1.5 mm. These findings highlight the sensitivity of active thermography to detect and map defects within specific size and depth ranges, although it faces limitations as the defect depth increases. Additionally, while it could identify the presence of defects, it struggled to accurately determine their shapes, whether circular

or square. Moreover, thermography gives an indication of the surface condition of the plate. Lines in the raw image represented in Figure 5 were observed across the entire plate, representing continuous carbon fibers. These observations further emphasize the thermography method's current capabilities and areas where it could be improved.

In contrast, the shearography technique exhibited lower sensitivity, detecting four defects out of the sixteen introduced in the composite plate made of 3D-printed material reinforced with continuous fiber. The defects identified were circular with diameters of 7 mm and 10 mm, located at a depth of 1 mm, and square with sizes of 7 mm and 10 mm, situated at a depth of 1.25 mm. Despite being able to detect these defects, shearography struggled to identify smaller defects, especially those at greater depths. The reliance on fringe pattern distortions to detect anomalies limits the clarity and precision of this method. The difficulty in interpreting shearographic images, combined with the subtlety of fringe pattern distortions, underscores the technique's challenges in providing comprehensive defect detection across varying depths and sizes within the material. Additionally, edge effects observed during wave propagation may distort the results and further reduce defect visibility near the boundaries of the plate.

Ultimately, active thermography has demonstrated a superior capability in identifying a higher number of defects, particularly those located near the surface and within a specific size range. While shearography was able to detect certain defects, especially those near the surface, its effectiveness could be significantly improved. The complementary use of both techniques could improve defect detection, especially in 3D-printed composite materials. However, further refinement of both methods is necessary to enhance their accuracy and reliability, particularly for detecting deeper or smaller defects within composite structures.

5. Conclusions

This study evaluated the feasibility and effectiveness of two NDT methods, active thermography and shearography, for detecting artificial defects in 3D-printed TP composites reinforced with continuous carbon fiber. The analysis revealed distinct strengths and limitations for each technique.

Active thermography demonstrated a higher sensitivity for detecting subsurface defects, particularly those within the size range of 3 mm to 10 mm and at depths of 1 mm and 1.25 mm in a 2.8 mm-thick 3D-printed composite plate. The post-processing techniques applied to the thermographic data significantly enhanced the visibility of defects, increasing the number of detectable defects from four to eight, thereby improving the method's overall detection capabilities. However, the technique faced challenges in identifying deeper defects beyond 1.5 mm and struggled to accurately determine the shapes of the detected anomalies.

Shearography, on the other hand, identified four defects, all located near the surface at depths of 1 mm and 1.25 mm. Despite its potential to detect near-surface defects, shearography's effectiveness was limited by its reliance on fringe pattern distortions, which proved difficult to interpret, especially for smaller or deeper defects. Additionally, edge effects and the complexity of analyzing wave propagation further limited the clarity of the results, reducing its reliability for detecting subtle or deep anomalies.

In summary, this study underscores the need for continued development and optimization of NDT methods tailored for 3D-printed composites reinforced with continuous fibers. The characteristics of these materials, including their internal structures and the presence of continuous fiber reinforcement, pose challenges for defect detection. Therefore, enhancing the sensitivity, accuracy, and interpretability of NDT techniques is essential for effectively identifying defects across varying depths and sizes within these composites. As the use of 3D-printed, fiber-reinforced composites expands in various high-performance applications, refining these testing methods will be critical to ensuring the reliability and safety of the materials in practical use.

Author Contributions: Conceptualization, A.D., A.N. and I.O.; methodology, A.D., A.N. and I.O.; validation, A.D. and F.D.; formal analysis, A.D., A.N. and I.O.; investigation, I.O.; data curation, A.N.

and I.O.; writing—original draft preparation, I.O.; writing—review and editing, A.D., A.N., F.D., M.K.H. and I.O.; visualization, A.D., A.N., F.D., M.K.H. and I.O.; supervision, A.D. and F.D.; project administration, A.D. and F.D.; funding acquisition, A.D. All authors have read and agreed to the published version of the manuscript.

Funding: The authors would like to thank Région Wallonne for supporting this research as part of the SKYWIN ICOM2C3D research project under grant 8820.

Data Availability Statement: Data are contained within the article.

Acknowledgments: The authors would like to thank the Wallonie Aerotraining Network for supporting this work.

Conflicts of Interest: The authors declare no conflicts of interest.

References

1. Cerniglia, D.; Montinaro, N. Defect Detection in Additively Manufactured Components: Laser Ultrasound and Laser Thermography Comparison. *Procedia Struct. Integr.* **2018**, *8*, 154–162. [CrossRef]
2. Lewis, G.K.; Schlienger, E. Practical considerations and capabilities for laser assisted direct metal deposition. *Mater. Des.* **2000**, *21*, 417–423. [CrossRef]
3. Azarov, A.V.; Antonov, F.K.; Vasil'ev, V.V.; Golubev, M.V.; Krasovskii, D.S.; Razin, A.F.; Salov, V.A.; Stupnikov, V.V.; Khaziev, A.R. Development of a two-matrix composite material fabricated by 3D printing. *Polym. Sci. Ser. D* **2017**, *10*, 87–90. [CrossRef]
4. Peters, S.T. *Handbook of Composites*, 2nd ed.; Chapman and Hall: London, UK, 1998.
5. Demarbaix, A.; Ochana, I.; Levrie, J.; Coutinho, I.; Cunha, S.S.; Moonens, M. Additively Manufactured Multifunctional Composite Parts with the Help of Coextrusion Continuous Carbon Fiber: Study of Feasibility to Print Self-Sensing without Doped Raw Material. *J. Compos. Sci.* **2023**, *7*, 355. [CrossRef]
6. Ahmed, O.; Wang, X.; Tran, M.-V.; Ismadi, M.-Z. Advancements in fiber-reinforced polymer composite materials damage detection methods: Towards achieving energy-efficient SHM systems. *Compos. Part B Eng.* **2021**, *223*, 109136. [CrossRef]
7. Ramírez, I.S.; Márquez, F.P.G.; Papaelias, M. Review on additive manufacturing and non-destructive testing. *J. Manuf. Syst.* **2023**, *66*, 260–286. [CrossRef]
8. Silva, M.I.S. *Non-Destructive Testing for Polymer Matrix Composites Produced by Additive Manufacturing*; Universidade Nova de Lisboa: Lisbon, Portugal, 2020.
9. Rus, J.; Gustschin, A.; Mooshofer, H.; Grager, J.-C.; Bente, K.; Gaal, M.; Pfeiffer, F.; Grosse, C.U. Qualitative comparison of non-destructive methods for inspection of carbon fiber-reinforced polymer laminates. *J. Compos. Mater.* **2020**, *54*, 4325–4337. [CrossRef]
10. Georges, M.; Srajbr, C.; Menner, P.; Koch, J.; Dillenz, A. Thermography and Shearography Inspection of Composite Hybrid Sandwich Structure Made of CFRP and GFRP Core and Titanium Skins. *Proceedings* **2018**, *2*, 484. [CrossRef]
11. Garnier, C.; Pastor, M.-L.; Eyma, F.; Lorrain, B. The detection of aeronautical defects in situ on composite structures using Non Destructive Testing. *Compos. Struct.* **2011**, *93*, 1328–1336. [CrossRef]
12. Wei, Y.; Xiao, Y.; Gu, X.; Ren, J.; Zhang, Y.; Zhang, D.; Chen, Y.; Li, H.; Li, S. Inspection of defects in composite structures using long pulse thermography and shearography. *Heliyon* **2024**, *10*, e33184. [CrossRef]
13. Hung, Y.; Chen, Y.; Ng, S.; Liu, L.; Huang, Y.; Luk, B.; Ip, R.; Wu, C.; Chung, P. Review and comparison of shearography and active thermography for nondestructive evaluation. *Mater. Sci. Eng. R Rep.* **2009**, *64*, 73–112. [CrossRef]
14. Saeed, N.; Abdulrahman, Y.; Amer, S.; Omar, M.A. Experimentally validated defect depth estimation using artificial neural network in pulsed thermography. *Infrared Phys. Technol.* **2019**, *98*, 192–200. [CrossRef]
15. Wei, Y.; Zhang, S.; Luo, Y.; Ding, L.; Zhang, D. Accurate depth determination of defects in composite materials using pulsed thermography. *Compos. Struct.* **2021**, *267*, 113846. [CrossRef]
16. Georges, M.P.; Vandenrijt, J.-F.; Thizy, C.; Alexeenko, I.; Pedrini, G.; Vollheim, B.; Lopez, I.; Jorge, I.; Rochet, J.; Osten, W. Combined holography and thermography in a single sensor through image-plane holography at thermal infrared wavelengths. *Opt. Express* **2014**, *22*, 25517–25529. [CrossRef] [PubMed]
17. Fu, Y.; Yao, X. A review on manufacturing defects and their detection of fiber reinforced resin matrix composites. *Compos. Part C Open Access* **2022**, *8*, 100276. [CrossRef]
18. Hung, Y.; Ho, H. Shearography: An optical measurement technique and applications. *Mater. Sci. Eng. R Rep.* **2005**, *49*, 61–87. [CrossRef]
19. Notebaert, A.; Quinten, J.; Moonens, M.; Olmez, V.; Barros, C.; Cunha, S.S.; Demarbaix, A. Numerical Modelling of the Heat Source and the Thermal Response of an Additively Manufactured Composite during an Active Thermographic Inspection. *Materials* **2023**, *17*, 13. [CrossRef] [PubMed]